JOURNAL OF APPLIED ELECTROCHEMISTRY 21 (1991) 95–98

AC impedance studies on nickel oxide electrodes to determine self-discharge characteristics of Ni–H_2 batteries

K. A. MURUGESAMOORTHI, S. SRINIVASAN, A. J. APPLEBY

Center for Electrochemical Systems and Hydrogen Research, 238 Wisenbaker Engineering Research Center, Texas Engineering Experiment Station, Texas A & M University System, College Station, TX-77843-3577, USA

Received 17 July 1989; revised 30 April 1990

AC impedance measurements were made on nickel oxide electrodes in an alkaline medium. The electrodes were prepared by electrodeposition of nickel oxide on nickel foils from a nickel nitrate solution. The main purpose of the investigation was to determine the dependence of impedance parameters on the state of charge of the electrode. The results demonstrated that the current phase shift and impedance modulus vary linearly with state of charge at low frequencies. Hence, the state of charge can be estimated from the values of phase shift and modulus. The state of charge of nickel electrodes exposed to argon and hydrogen was determined at various time intervals. It was found that the electrode exposed to hydrogen discharged faster than that exposed to argon, indicating that hydrogen enhances the self-discharge rate of nickel oxide electrodes.

1. Introduction

Nickel oxide electrodes have been extensively studied by many researchers for decades because of their applications in a variety of batteries [1–6]. They are used as the positive electrode in nickel-iron, nickel-zinc, nickel-cadmium and nickel-hydrogen systems. Nickel-hydrogen batteries exhibit long cycle life, high depth of discharge, high energy density, and tolerance to over-charge and over-discharge. Because of these advantages, nickel-cadmium batteries have been widely displaced by nickel-hydrogen batteries in space applications.

The main disadvantage of the nickel-hydrogen battery is its high self-discharge rate, of about 10% per day, which is about five to ten times higher than that of the nickel-cadmium battery. The most probable reason for this self-discharge is the reduction of nickel oxide from the trivalent to the divalent state by hydrogen. Hydrogen is stored under high pressure in the battery: typically is about 3 MPa in the discharged state and about 10 MPa in the charged state. The design of the single cell and of the multi-cell stack in a typical nickel-hydrogen battery has been described elsewhere [7]. To evaluate self-discharge, the fact that hydrogen can reach the nickel electrode externally and/or through the electrolyte must be considered.

AC impedance is a promising technique to determine the state of charge of a battery. A small AC signal, as low as 5 mV, causes only a minor perturbation to the system under study. When DC techniques are used, the perturbation is much greater. Another advantage of the AC techniques is that it can provide more information. However, because of the complexity of instrumentation, and the time involved in carrying out measurements over a wide frequency range, it has not been widely used until recently.

The impedance and mass transport kinetics of nickel-cadmium cells have been studied by Zimmerman *et al.* [8] in the frequency range 0.0001 to 100 Hz. Two diffusion process were observed in the impedance spectrum. Lenhart *et al.* [9] used the method to elucidate the degradation of porous nickel battery electrodes, using transmission line models to represent their impedance. The state of charge of a battery or an electrode is the ratio of the residual capacity at a given instant to the maximum capacity available. The state of charge of nickel-cadmium [10] and lead acid batteries [11] have been correlated with impedance parameters.

In this paper, an attempt is made to understand the self-discharge mechanism of nickel-hydrogen batteries by determining the AC impedance characteristics of nickel oxide electrodes exposed to hydrogen. For this purpose, fully charged electrodes were exposed to hydrogen (or argon in control experiments) in an alkaline medium under open circuit conditions. Impedance measurements were carried out after various times from end of charge.

2. Experimental details

2.1. *Deposition of nickel oxide electrodes*

Nickel oxide electrodes were prepared by electrochemical deposition onto nickel foils. Nickel foils (Alfa products – 99.998% purity) of 0.127 mm thickness were used as electrodes after applying an anodic cur-

0021-891X/91 $03.00 + .12

rent of 10 mA cm^{-2} for about one minute in 1 M HCl, rinsed with acetone, then with deionized water. Nickel nitrate (2 M) plus ethanol (60 : 40 by volume) was used as the electrolyte. Electrodeposition was carried out by applying a cathodic current of 35 mA cm^{-2} at the boiling point of the solution (80° C) for 90 min.

2.2. *Electrodes pretreatment*

The nickel oxide electrodes were pretreated as described below before measurements. After deposition, the electrode was washed with deionized water. The electrode was weighed and its capacity was calculated to be 10 mAh from the amount of nickel oxide deposited, assuming that the one-electron transfer reaction $Ni(OH)_2$ to NiOOH applied. The electrode was charged at the $C/5$ rate for one hour, which was followed by discharge at the $C/2$ rate to 1 V against Zn/ZnO. This process was repeated three times.

2.3. *Electrochemical measurements*

The charge-discharge cycles and the AC impedance studies were made on the nickel oxide electrodes in 30% KOH (analytical grade); a platinum spiral and a zinc wire were used as the counter and reference electrodes respectively. The reference electrode was isolated from the solution by means of a Luggin capillary. Ultrapure argon or hydrogen was bubbled through the solution. AC impedance measurements were made using an EG & G Model 273 Potentiostat/Galvanostat, a Model 5301A Lock-in-Amplifier and a Model 5315 preamplifier, coupled with an IBM-PC, in the frequency range 5 Hz to 60 KHz. Measurements were made at room temperature (20° C), and were not made at low frequencies because of the effect of the signal on electrode potential and the change in the state of charge during the period of the measurements.

3. Results and discussions

Figure 1 shows the Nyquist plot for the nickel oxide electrode in the fully charged state (1.9 V against Zn/ZnO), when exposed to argon. At high frequencies the plot starts as a semicircle, and as frequency decreases it changes to a straight line having an angle of 45° with the real axis. When the frequency further decreases the angle increases, indicating capacitive behaviour. However, after self-discharge (i.e., with the electrode left on open circuit for varying times after charging), the initial curvature slowly decreases and only a straight line with a slope of 45° was observed, indicating a pure diffusional behaviour. The intercept of the plot at high frequencies on the resistance axis gives the value of the solution resistance between the working and the reference electrodes, which was found to be 48 Ω. Data for this intercept were recorded after leaving the electrode at open circuit for varying periods of time after the end of charge. Similar experiments were then carried out in a hydrogen gas atmosphere. Figure 2 represents the equivalent circuit used to represent the processes occurring at the nickel oxide electrode to assist in analysing the impedance data. R_{so}, C_{dl}, R_{ct} and W are the solution resistance, double layer capacitance, charge transfer resistance and the Warburg impedance, respectively.

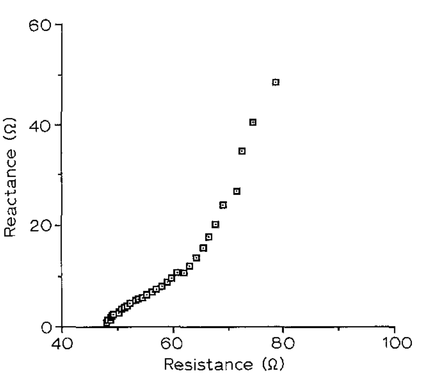

Fig. 1. Nyquist plot of the nickel oxide electrode in fully charged state (1.9 V against Zn/ZnO) under Argon atmosphere and at 20° C.

The properties of the Randles type impedance network shown in Fig. 2 have been extensively examined in the literature [12]. The total impedance, Z, of any network is given by

$$Z = R_s - \left(\frac{j}{\omega C_s}\right) \tag{1}$$

where R_s, C_s are the effective series resistance and capacitance respectively of the above network, and ω is the angular frequency. The series resistance R_s may be expressed by [10]

$$R_s = R_{so} + \left(\frac{R_{ct} + \sigma/\sqrt{(\omega)}}{(1 + \sqrt{(\omega)}C_{dl}\sigma)^2 + \omega^2 C_{dl}^2 (R_{ct} + \sigma/\sqrt{(\omega)})^2}\right) \tag{2}$$

The capacitance is given by [10]

$$\frac{1}{\omega C_s} = \left(\frac{(\sigma/\sqrt{(\omega)})(1 + \sqrt{(\omega)}C_{dl}\sigma) + \omega C_{dl}(R_{ct} + \sigma/\sqrt{(\omega)})^2}{(1 + \sqrt{(\omega)}C_{dl}\sigma)^2 + \omega^2 C_{dl}(R_{ct} + \sigma/\sqrt{(\omega)})^2}\right) \tag{3}$$

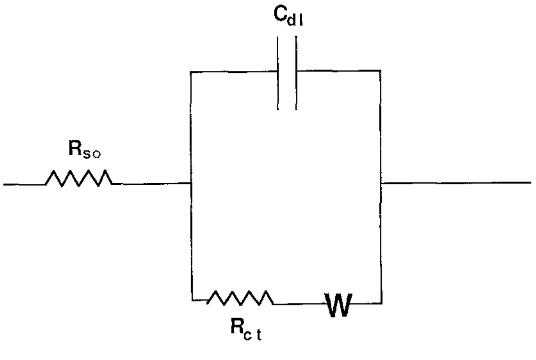

Fig. 2. Equivalent circuit of the nickel oxide electrode for the impedance spectrum.

where

$$W = \left(\frac{\sigma}{\sqrt{(\omega)}} - \mathrm{j}\frac{\sigma}{\sqrt{(\omega)}}\right) \tag{4}$$

and σ the Warburg coefficient.

The expression for the Warburg coefficient includes terms containing the concentrations of the reactants and products, as well as their diffusion coefficients. The charge transfer resistance, R_{ct}, is related to the concentration term through the exchange current density, since

$$R_{ct} = \left(\frac{RT}{nFI_0}\right) \tag{5}$$

where R is the gas constant, T is the absolute temperature, F is the Faraday constant, n is the number of electrons involved in the reaction and I_0 is the exchange current density. The impedance parameters will vary according to the concentration of the reacting and the product species, hence on the state of charge of the electrode. The variation in the impedance parameters with state of charge of the electrode will be prominent in the low frequency region, because the parameters σ and R_{ct} are observed here.

The fully charged electrode had a capacity of 10 mAh, from which a predetermined amount of charge was withdrawn by discharge at constant current at the $C/10$ rate after which the state of charge was calculated. After a desired period of time the a.c. impedance was measured. This was repeated for different states of discharge. The variations of parameters such as impedance modulus, current phase shift, and series resistance were analysed with respect to the state of charge of the electrode. The current phase shift and the impedance modulus were found to vary significantly with state of charge at low frequencies. However, at high frequencies there was no appreciable change of these parameters with state of charge. No particular trend in the variation in the series resistance with state of charge was noted. Figure 3 shows the variation of current phase shift with state of charge at three different frequencies. At all three frequencies, the variation was almost linear. The variation of phase angle with the state of charge was similar to that for the nickel-cadmium cell [10]. Figure 4 shows the variation of the impedance modulus with state of charge at four different frequencies. The variation of the modulus with state of charge at 5 Hz is close to linear, compared to those at other frequencies.

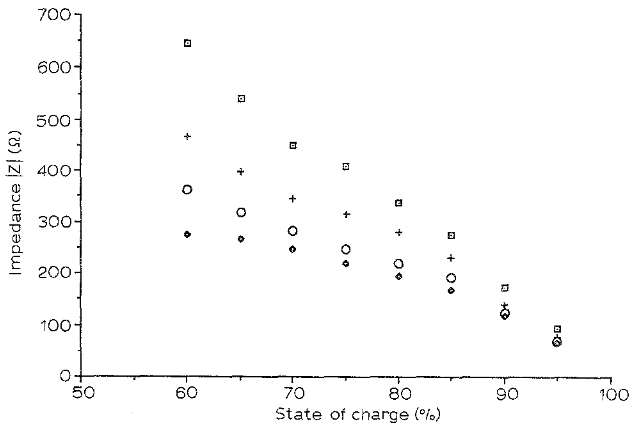

Fig. 4. Variation of impedance modulus |Z| with state of charge of the nickel oxide electrode in 30% KOH at 20° C and at (□) 5 Hz, (+) 10 Hz, (O) 20 Hz, and (◇) 30 Hz.

Hence, variations of the phase shift and the impedance modulus could be used for the estimation of the state of charge of the electrode. The open circuit potential was monitored as a function of time when the fully charged electrode was exposed to argon or hydrogen. Figure 5 shows the open circuit potential (Zn/ZnO reference) against time, when the charged electrode is left in KOH under one atmosphere of argon or hydrogen. It is evident from the plots that the open circuit potential of the electrodes in both cases decreases with time. After a certain time, the open circuit potential of the electrode exposed to hydrogen is less than that exposed to argon, however, monitoring this potential does not give any quantitative measure of the state of charge of the electrode. The AC impedance measurements were performed at different time intervals after the fully charged electrodes were immersed in KOH under an argon or hydrogen atmosphere. The states of charge of the electrodes were estimated from the values of the impedance modulus and of the phase angle at 5 Hz.

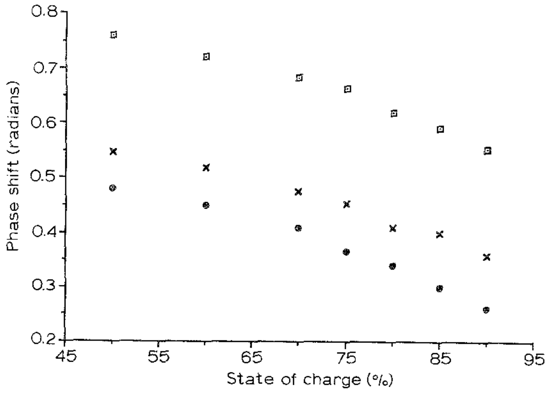

Fig. 3. Variation of phase angle and the electrode impedance with state of charge of the nickel oxide electrode in 30% KOH at 20° C and at (□) 5 Hz, (×) 10 Hz, and (●) 20 Hz.

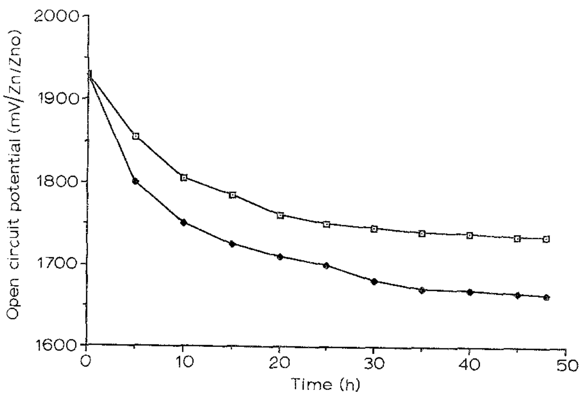

Fig. 5. Plot of open circuit potential of the electrode against time when the electrode in 30% KOH is exposed to argon (□) or hydrogen (◆) at 20° C.

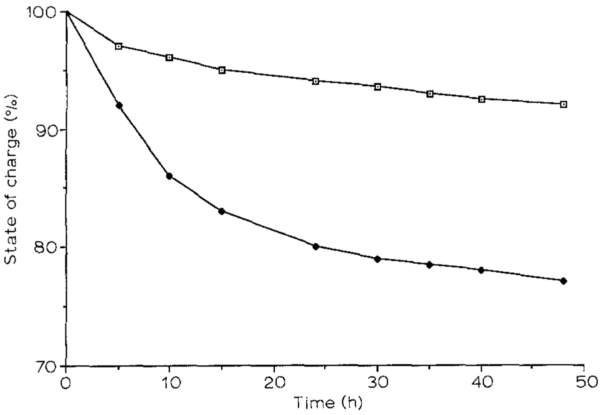

Fig. 6. Plot of state of charge of the electrode against time when the electrode in 30% KOH is exposed to argon (□) or hydrogen (◆) atmosphere at 20° C.

Figure 6 shows the plots of the state of charge as a function of time when the electrode was exposed to argon or hydrogen, respectively. The states of charge were estimated using the values of phase shift at 5 Hz from Fig. 3. There was no significant deviation when these were estimated from the variation of modulus (Fig. 4). As shown in the plots in Fig. 6, after any particular time from the fully charged state, the state of charge of the electrode exposed to hydrogen is much lower than that exposed to argon. Hence, it is clear that hydrogen causes the self-discharge of the nickel oxide electrode, hence that of the nickel-hydrogen battery. Measurements with battery electrodes at different hydrogen pressures are continuing. A possible reaction which causes the self-discharge of nickel oxide electrodes may be represented by the overall reaction:

$$NiOOH + \tfrac{1}{2}H_2 \longrightarrow Ni(OH)_2 \qquad (6)$$

which can take place in the two electrochemical steps

$$NiOOH + H_2O + e^- \longrightarrow Ni(OH)_2 + OH^- \qquad (7)$$

and

$$\tfrac{1}{2}H_2 + OH^- \longrightarrow H_2O + e^- \qquad (8)$$

4. Conclusions

The state of charge of a nickel oxide electrode can be predicted from the variation of the phase shift and that of the impedance modulus at low frequencies. The states of charge of electrodes were estimated after given times from the fully charged state. The state of charge of electrodes decreases much faster when exposed to hydrogen, than when they were under argon atmosphere indicating that the presence of hydrogen results in self-discharge of the electrode.

References

[1] B. E. Conway and P. L. Bourgault, *Can. J. Chem.* **37** (1959) 292.

[2] B. E. Conway and M. A. Sattar, *J. Electroanal. Chem.* **19** (1968) 351.

[3] M. A. Sattar and B. E. Conway, *Electrochim. Acta* **14** (1969) 695.

[4] S. U. Falk and A. J. Salkind, 'Alkaline Storage Batteries', Wiley & Sons, New York (1969).

[5] G. W. D. Briggs, 'A specialist Periodical Report: Electrochemistry' Volume-4, The Chemical Society Burlington House, London (1974) pp. 33–54.

[6] R. Barnard, G. T. Crickmore, J. A. Lee and F. L. Tye, *J. Appl. Electrochem.* **10** (1980) 61.

[7] C. A. Vincent, 'Modern Batteries', Edward Arnold, London (1984).

[8] A. H. Zimmerman, M. R. Martineli, M. C. Janecki, C. C. Badcodk, *J. Electrochem. Soc.* **129** (1982) 289.

[9] S. J. Lenhart, D. D. Macdonald and B. G. Pound, *ibid.* **135** (1988) 1063.

[10] S. Sathyanarayana, S. Venugopalan and M. L. Gopinath, *J. Appl. Electrochem.* **9** (1979) 125.

[11] M. L. Gopinath and S. Sathyanarayana, *J. Appl. Electrochem.* **9** (1979) 369.

[12] M. Sluyters-Rehbach and J. H. Sluyters, 'Electroanalytical Chemistry', Vol. 8 (edited by A. J. Bard), Dekker, New York (1971) p. 157.